Development and Demonstration of an Optical Autocovariance Direct Detection Wind Lidar

Christian J. Grund, Sara Tucker, Robert Pierce, Miroslaw Ostasziewski, Kelly Kanizay, Dina Demara, Jim Howell
Ball Aerospace & Technologiew Corp.
1600 Commerce St.
Boulder, CO 80301
cgrund@ball.com

Abstract— **The 3-D winds mission will fulfill critical currently unmet environmental sensing needs identified in the NASA Decadal Survey [1]. We report on progress in the development and validation of an airborne Optical Autocovariance Wind Lidar (OAWL) that uses a unique interferometric receiver and direct-detection to efficiently and accurately measure the profiles of wind speed by resolving the optical Doppler shift of backscatter from a pulsed laser. A three year ESTO-funded IIP is in progress to build a complete OAWL lidar system, and flight test from a WB-57 aircraft, exiting at technology readiness level TRL-5 by 2011. The flight data will be used to validate engineering models that predict space-borne system performance. The current baseline "hybrid" 3D winds sensor approach requires two lidars: a low resolution direct-detection double-edge etalon system operating at 355nm measuring the molecular backscatter component, and 2 μm wavelength coherent detection system capturing the aerosol component. The OAWL approach enables a simpler, lower mass alternative architecture that uses a single laser and wavelength system to provide the needed measurements. In this paper, we discuss IIP program objectives, OAWL performance expectations in airborne and space deployments, system design, and fabrication status, vibration testing, and validation experiment design.**

Keywords-component; Lidar; Doppler wind lidar; Optical autocovariance; 3D winds mission

I. INTRODUCTION *(HEADING 1)*

Winds are key dynamic drivers of the atmospheric mass and energy fields. Insufficiencies and inaccuracies in current wind observations, particularly over the oceans, in the southern hemisphere, and in the tropics, lead to uncertainty in the modeling of global atmospheric circulations, limiting weather forecasting accuracy and diminishing our understanding of water, chemical species, and energy transport. The NASA Decadal Survey specifically states that: Tropospheric winds are the number one unmet measurement objective for improving weather forecasts, and defines a 3-D Winds mission that identifies Doppler Wind Lidar (DWL) in low earth orbit (LEO) as the key technology needed to meet the global wind profiling objectives[1]. To profile winds, DWL's measure the line of sight optical Doppler frequency shift from aerosols and molecules as a function of range. Backscatter from molecules is ever-present but spectrally broadened by thermal motions diminishing the achievable wind measurement precision. Aerosols produce insignificant backscatter spectral broadening providing the best wind information, but are not always present. A hybrid lidar [2] measuring winds from both aerosol and molecular backscatter therefore maximizes the availability of wind profiles. The Optical Autocovariance Wind Lidar (OAWL) [3] is a direct detection DWL approach that uses a unique high resolution (10^9) interferometer to measure line-of-sight (LOS) aerosol backscatter winds to <0.5 m/s precision. When operated at UV wavelengths (~355nm), OAWL can simultaneously measure molecular and aerosol backscatter winds; however, a more photon-efficient Integrated Direct Detection (IDD) architecture employs a dual-edge etalon pre-filter to separately measure the Doppler offset of the molecular fraction of the backscatter return, while leaving the aerosol-backscatter-dominated center of the Doppler shifted spectrum for analysis by the high resolution OAWL. The IDD hybrid approach uses a single transmit laser and receiving system with relaxed 1-wave telescope optical requirements, making it much simpler, lower mass, lower cost, and more power efficient than the alternative hybrid approach that uses a combination of a 2 micron Coherent Detection DWL [4] for aerosol wind profiling combined with a separate 355nm dual-edge etalon direct detection DWL [5] for measuring the molecular component. This paper discusses the development and demonstration of the OAWL DWL system under NASA ESTO IIP funding; we are in the second year of the three year program. The primary objectives of the IIP are to raise the OAWL DWL technology from TRL3 to TRL5 by taking the multi-wavelength field-widened OAWL receiver built under Ball internal funds, integrating it into a complete lidar system (telescope, laser, data system, framework) configured to fit in a WB-57 aircraft palate, ground validate the OAWL system against a coherent Doppler lidar, and then validating the system performance from the WB-57 against wind profilers and a ground-based coherent DWL system.

II. OAWL THEORY

The typical spectral distribution of monochromatic light backscattered from the atmosphere is shown in Fig. 1(top) as a function of the wavelength shift expressed in terms of the LOS wind velocity V. For optical wavelength λ, the relationship between the optical Doppler shift frequency Δf and the velocity V is given in (1).

$$\Delta f = V/\lambda \quad (1)$$

The Optical Autocovariance Function (OACF) expected from a typical return spectrum as a function of Optical Path Difference (OPD) between the legs of the interferometer (e.g. a Michelson or Mach-Zehender) is shown in Fig. 1 (bot). For a specific fixed interferometer OPD, the Doppler shift of the return spectrum due to the line of sight (LOS) wind velocity, V, is calculated from $\Delta\phi$, the OACF phase shift, (here expressed as a fraction of an OACF cycle), according to (2).

$$V = \lambda * \Delta\phi * c / (2*OPD) \quad (2)$$

where c is the speed of light, and λ is the wavelength. Because the OACF is a periodic function, there is a finite unambiguous velocity interval given by (3).

$$\Delta V = \pm\lambda c/(2*OPD) \quad (3)$$

In practice, $\Delta\phi$ is determined by fitting a sine function to a sample of the transmitted pulse to determine a 0-velocity phase baseline and calculating the OACF phase difference to the sine fit of the received light. The sine fits are performed on several intensities simultaneously measured at OPD's sequentially differing by $\lambda/4$ (denoted CH1-CH4 in Fig. 1 (bot)). Measuring $\Delta\phi$ as a differential from every transmitted laser pulse allows the OAWL system to operate open-loop by eliminating sensitivity to thermal drift of the receiver and pulse-to-pulse laser wavelength jitter that would otherwise require complex and costly active control systems.

Beyond winds, for large OPD's the amplitude (A) of the resolved coherent part of OACF is a measure of the aerosol dominated center of the spectrum, while the sine fit offset (Θ) is a measure of the remaining spectrum arising from the unresolved molecular backscatter component of the return. This separation of components enables simultaneous retrieval of winds and extinction corrected aerosol backscatter profiles by the High Spectral Resolution Lidar (HSRL) method [3]. Calibrated aerosol retrievals are of interest for climate studies, and are directly applicable to other critical Decadal Survey missions such as ACE and GACM.

As suggested by Fig. 1(bot), choosing OPD's <100 mm, both aerosol and molecular parts of the spectrum can be simultaneously measured. Modeling has shown that the improved SNR does not compensate for the loss in velocity precision afforded by longer OPD's (>0.5m). It is more efficient to measure the molecular component separately, as by using a complimentary double-edge etalon filter receiver [5].

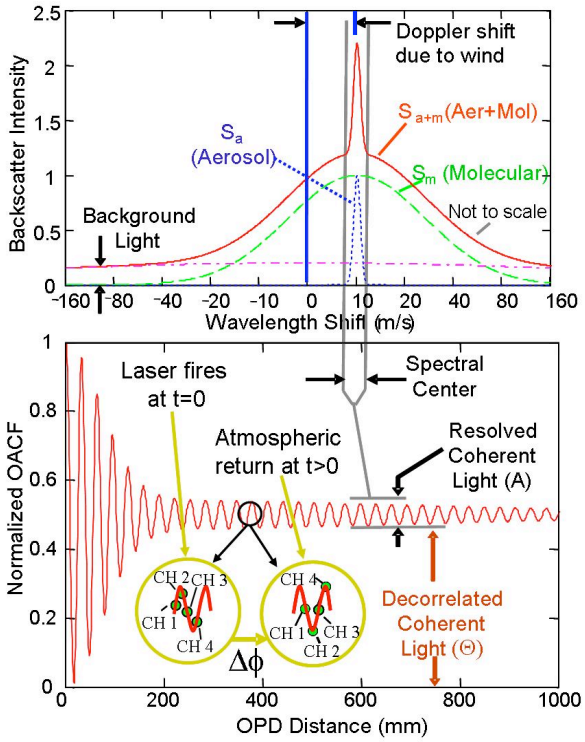

Figure 1. (Top) The optical spectrum of the backscattered light from a monochromatic source (at 0 wavelength shift) is a linear sum of the near-monochromatic aerosol backscatter and the Doppler-broadened molecular backscatter. The center frequency of return is altered by the Doppler shift due to the wind. (Bot) The amplitude envelope of the OACF of the backscatter spectrum is a function of the signal strength, spectral width, and the OPD. The frequency of the OACF is determined by the optical signal frequency. The phase shift of the OACF is proportional to the OPD*optical frequency, enabling high resolution of small optical frequency shifts.

III. OAWL System Implementation

A. *Fundemental OAWL Proof of Concept*

Under Ball internal funding, a fundamental laboratory proof of concept (POC) OAWL lidar system was demonstrated in 2007 [6]. This system employed a low power 523nm frequency-doubled Nd:YLF laser transmitter and 150mm diameter receiver optics suitable for short range atmospheric measurements. The laser used an uncontrolled intra-cavity etalon to force mostly single mode operation, but exhibited frequent shot-to-shot mode hops. The receiver implemented three ~λ/4 parallel interferometer paths with common component substrates using flat mirror optics. The fixed OPD's differences were implemented by coating three zones with different reflective coating thicknesses on one of the interferometer mirrors (architecture due to Schwiesow [7]).

The POC system produced ~1m/s precision with 3m range resolution and 0.3s time as compared to a co-located sonic anemometer. Successful wind measurements despite the frequent laser mode-hops also demonstrated the efficacy of the 0-velocity laser sampling strategy.

NASA ESTO IIP funding for this work is gratefully acknowledged under grant NNX08AN36G

B. Flight-path multi-λ field-widened receiver

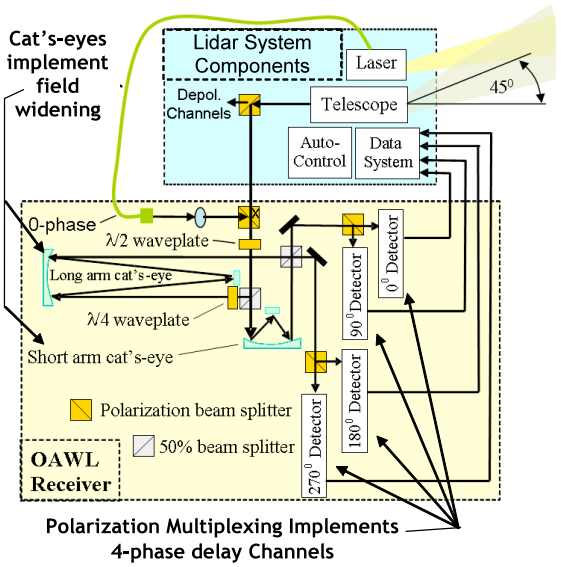

Figure 2. Architecture of the achromatic, field-widened OAWL receiver (yellow background). The components shown with teal background are required to complete an OAWL Doppler wind lidar system and have been added under the NASA IIP program.

Based on our experiences with the POC system, and with a view toward a flight-path that also enables multiwavelength HSRL measurements, Ball designed and fabricated an OAWL / OA-HSRL, field-widened, multi-wavelength receiver suitable for aircraft testing. The receiver architecture is shown in Figure 2.

This design implements a unique Mach-Zehender-like interferometer that incorporates offset beam path cat's eye reflectors to enable field-widened operations with a 1m OPD. An achromatic λ/4 waveplate is inserted in one leg of the interferometer to create quadrature phase delays, and polarization multiplexing allows the simultaneous use of the same interferometer path fully overlapped on all optical surfaces for all four OACF phase delay channels. The polarization multiplexing approach is similar to that shown by Bruneau [8], however the unique cat's-eye field-widening architecture provides a path to practical space implementations using heritage telescope and optical components (e.g. CALIPSO [9]). The cat's-eye construction relaxes the stringent requirement for receiver/transmitter alignment and small field of view (FOV) needed to achieve similar resolution with non-field widened approaches, such as employed in the ALADIN instrument on the European ADM wind mission [10], and results in a smaller volume requirement for the intereferometer for a given size telescope..

Though not shown in Figure 2, on exiting the interferometer, in the actual receiver, a dichroic mirror allows separation of two wavelength signals into different paths before the final polarization beamsplitters. Narrowband filters are placed in the separated paths to minimize background light. While only one λ is needed for winds, the accommodation for

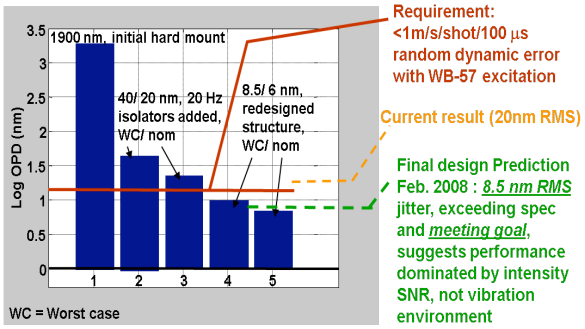

Figure 3 Progressive improvement of the OAWL receiver during the iterative design process using the EOSyM integrated model. The ordinate is given in nm RMS jitter that is linearly related to LOS measurement error. The IIP program requirement level with a margin assumption of 6X is shown in red (12 nm RMS, equivalent to ~1m/s/shot/100 μs); the model prediction for performance of the final design (8.5nm RMS) is shown in green. The RMS OpVibe-level results from the receiver tests on a vibe table are shown in yellow. Even though the actual measured jitter exceed the predicted jitter by ~2.4, it is still well within the requirements margin needed for successful IIP flight tests that will average ~2000 laser returns/profile..

simultaneous operation at 355nm and 532 nm provides an opportunity for future multi-wavelength HSRL backscatter and extinction measurements demonstrations for aerosol studies and combined wind-aerosol retrievals. Also accommodated is the ability to separately measure the depolarized component of the return. This is useful for discrimination of ice from water clouds and provides insight into aerosol particle microphysics. The depolarization signals are measured by two additional detectors filtered for each of the wavelengths (not shown). These detector channels do not participate in the wind measurements, and use light otherwise rejected by the OAWL system, so also do not interfere with wind measurement performance. Although, a single-mode fiber is shown conducting a sample of the outgoing laser light into the interferometer for the 0-time, 0-phase, 0-velocity reference, the IIP system employs direct coupling in a similar manner.

C. OAWL Receiver Vibration Testing

During the receiver design phase, the Ball EOSyM integrated modeling system was used to evaluate the expected performance under aircraft vibration loads. For this application, EOSyM was configured to accept the optical model and the mechanical solid model of the receiver, and the measured PSD for the WB-57 aircraft [11]. The model predicts the intensity, contrast and OACF phase jitter effects caused by both aircraft vibration within the lidar return time (~100 μs) and the thermoelastic response. **Error! Reference source not found.** shows the time history of the model predictions as we iterated the design of the receiver baseplate, optical mount stiffnesses, and mounting isolation to achieve the design goals.

*

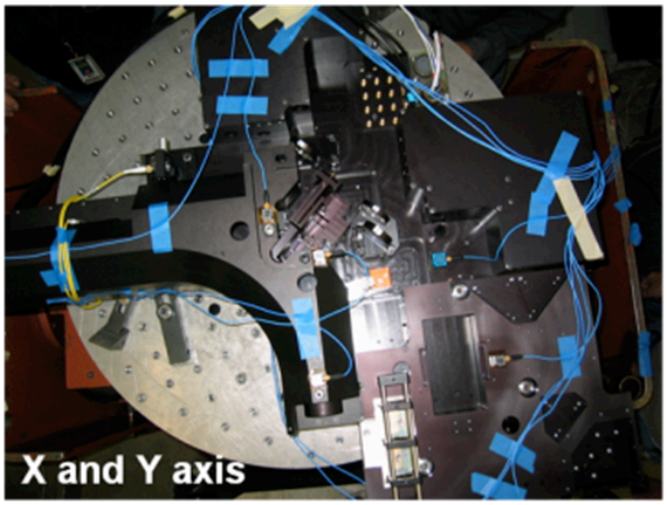

Figure 4 The OAWL receiver is shown mounted to the vibe table in the Ball vibe lab. The blue wires conduct signals from multiple accelerometers. Accelerometer data and interferometer signal data were recorded simultaneously. The receiver input aperture was illuminated by a single frequency 532nm CW laser during these tests.

After adding appropriate isolators, only a single design turn was needed to exceed the 8.6 nm requirements, resulting in a predicted vibration induced error of <6nm OPD jitter in 100 μs. (equivalent to ~0.5 m/s RMS error per shot). In operation, each wind profile is expected to comprise an average over ~2000 laser shots.

Prior to delivering the actual OAWL receiver for integration into the OAWL IIP lidar system, we subjected it to vibration testing for both WB-57 aircraft operational levels (Opvibe. 0.08 gRMS), and to taxi-takeoff-and landing levels (TTOL, 1.78 gRMS) to ensure workmanship and that the interferometric level alignments would not be affected. The OAWL receiver is shown mounted to the vibe table in Fig. 4.

Results of the Opvibe tests are also plotted in Fig. 3 in yellow. Vibration-induced OPD jitter of the observed 20 nm RMS is expected to result in <0.03 m/s wind profile error, inconsequential compared to the few tenths of m/s program validation goals, and small compared to the ~0.1 m/s errors in velocity resulting from the expected return intensity signal-to-noise ratio (SNR).

The system not only survived the TTOL tests, but demonstrated a useful level of wind measurement performance can be expected even during environmental conditions resulting in the harsher TTOL vibration levels.

Since this analysis, several factors affecting the model prediction fidelity have been uncovered including non-linear detector effects and that the locations modeled for the optics do not exactly coincide with the accelerometer locations during the test. Model validation is still in progress, and incorporating these effects is expected to reduce the apparent discrepancy between the model and the predicted performance.

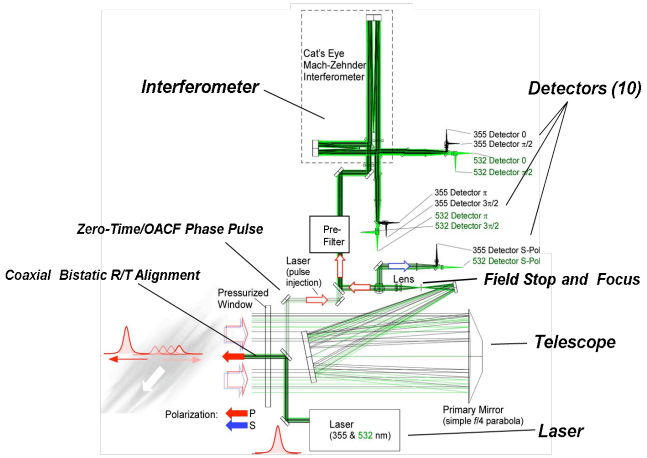

Figure 5 The OAWL IIP system architecture and major components.

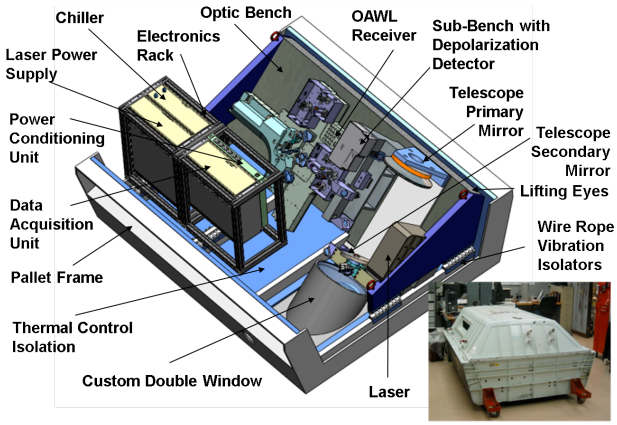

Figure 6 Solid model of the layout of the OAWL System in the WB-57 pallet showing the key components. Lower right: Actual pallet.

IV. The OAWL IIP DWL System

A. IIP System Architecture

The architecture of the complete OAWL DWL system built for the IIP is shown in Fig. 5. The laser is in procurement from a commercial company from a flight heritage design. It develops 30 mJ/pulse at 355nm, and 16 mJ/pulse at 532nm at a 200 Hz pulse repetition rate, sufficient for IIP testing, and for model validation.. Pulse widths are ~18 ns. The receiver telescope is ~300 mm.

The arrangement of components in the WB-57 pallet is shown in Fig. 6. The pallet is pressureized to 5 PSI when flying at altitude. A photo of the actual pallet is shown in the inset. To keep the window thickness (and cost) under control, a double window arrangement was employed with the pressure between windows equalized with the outside air pressure. Bowing of the inner window with differential pressure is unimportant because it is normal to the optical beam. The WB-57is scheduled to fly at ~15km altitude for the tests.

*

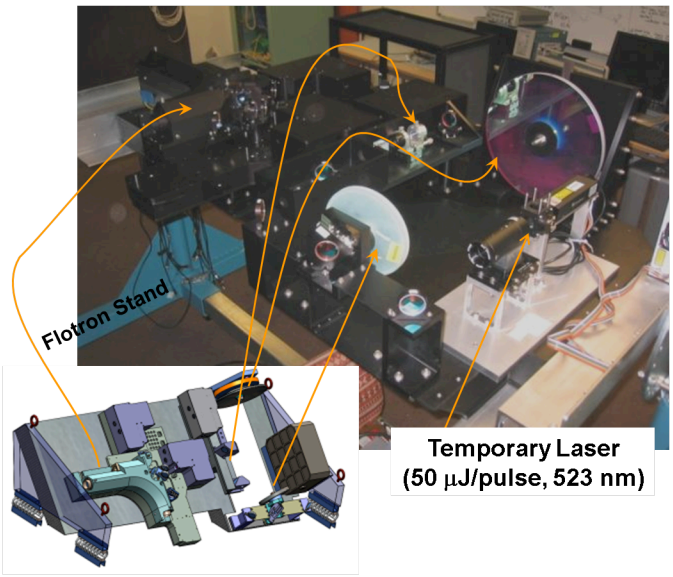

Figure 7 shows the completed IIP DWL transceiver system (except for the delinquent laser) supported by a Flotron stand in the rooftop instrument testing facility at Ball. The facility provides easy access for open air testing. The solid model insert identifies some of the components.

B. The IIP data system

The data system is constructed around a standard PXI chassis to which we have attached auxiliary cooling fans to increase air flow at altitude. Each detector channel uses a multi-pixel photon counting detector (MPPC) that is suitable for recording the large but brief 0-velocity pulse as it is emitted, while having the capacity to record the time delayed atmospheric returns with photon-counting sensitivity. Each custom detector module includes electronic circuits that bias the individual detectors and provide both digital photon counting outputs and analog outputs that allow tracking the many-simultaneous photon signals from the 0-velocity pulse and from clouds and the ground, for instance. The data system therefore has a custom data acquisition card that has been designed to handle and synchronize the large number of detector channels. The card supports a high performance FPGA to keep power dissipation and volume under control. This card has been fabricated, integrated into the system, tested.

In addition to the custom acquisition card, the PXI chassis supports a master controller, low speed analog ADC (e.g. for temperatures, accelerometers, and voltage monitoring). An AIRINC interface for acquisition of geolocation, attitude and other aircraft information provided by the WB-57 platform, a solid-state hard disk that stores the acquired data and the data system power supply.

C. IIP Hardware status

The IIP system hardware is complete and ready for ground testing with the exception of the specified laser that has been delayed by the vendor for 5 months at this writing due to multiple issues meeting requirements. These issues included pulse width and spectral bandwidth, optical damage, and polarization state. However, we are expecting the laser within the next few weeks. In the interim, we have installed the small laser that was used in the original 523nm wavelength POC system so that we could continue with system shake-out testing, and acquire some short range wind profiles. This laser worked long enough for us to establish that the system is well aligned and functions as a lidar, and that the data system is functional. Unfortunately, that laser failed within a few hours of operation, precluding us from acquiring atmospheric wind data. We then found a brand new single longitudinal mode 532nm pulse laser within the company, and proceeded to test it to see if it would be suitable for preliminary OAWL operation. Unfortunately, it was found to have a bad controller (right out of the box), so it is in repair (in Germany) at this writing.

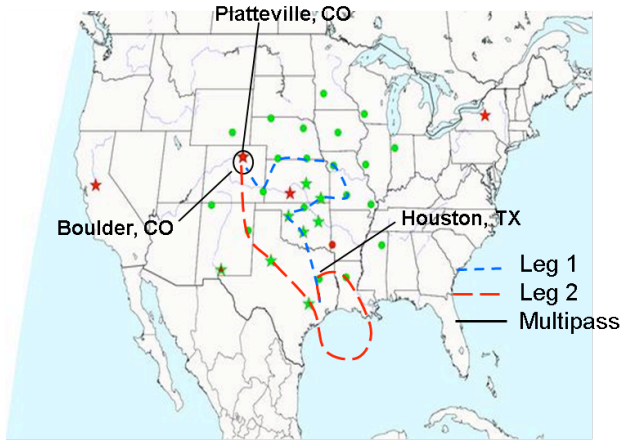

Figure 8 The airborne test plan the OAWL IIP system includes flights out of Houston to and from Boulder, CO, circling many wind profilers in the NOAA network. The flight path will cover a variety of terrain and ocean backgrounds, hopefully providing observations under different cloud conditions. Higher temporal and spatial resolution profiles will also be provided by a coherent detection DWL systems in the Boulder area..

Fig. 7 shows the pallet system in a rooftop lab supported by a Flotron stand that allows pointing the system at any elevation or azimuth angle for ground testing.

V. IIP Test Plans

After the shake-out testing is complete the IIP program calls for two rigorous testing and validation periods. The first validations will be provided by ground testing alongside the well characterized NOAA mini-MOPA coherent detection DWL system. These tests will be conducted at the NOAA Table Mountain facility just north of Boulder, CO. The ground testing preparation are complete and the schedule is only pending receipt and integration of the correct laser.

In the Fall of 2010, we plan to execute the high altitude flight tests that will result in raising the OAWL technology to TRL-5. An overview of the flight test plan is given in Fig. 8. The plan includes flights out of Houston to and from Boulder, CO, circling many wind profilers in the NOAA network. The system does not include a scanner, so the flight path will carry the beam path (nominally 45° to vertical) about each profiler simulating a scan and allowing the vector wind profile to be derived. The flight path will cover a variety of terrain and ocean backgrounds, providing observation opportunities under different cloud conditions. Higher temporal and spatial resolution profiles will also be provided by one of the NOAA coherent detection DWL systems in the Boulder area during overflights.

VI. Next Steps

For the WB-57 flight tests, the data system has to collect geolocation and attitude information provided by the WB-57 platform via an AIRINC interface, as well as housekeeping and health and status data from the instrument itself including a backup accelerometer to determine the OAWL attitude. For the flight tests, the system must. run in a fully autonomous mode. Significant effort will be dedicated to testing operations over all conceivable flight conditions including brief and extended power outages. Once completely populated, the PXI chassis with its booster fan assembly will be tested at 5 PSI ambient with a set of temperature sensors affixed in critical locations to ensure overheating will not be a problem. Final assembly of the system in the pallet will include air ducting plenums and installation of auxiliary heating and cooling capability in the laser water cooling loop. In the event of complete power failure to the pallet, insulation and thermal mass are sufficient to keep the system above survival temperature for at least 1 hour while the plane descends and lands.

VII. Conclusions

An complete OAWL wind lidar system has been built that is suitable for aircraft testing and incorporates in a demonstrable way many of the system design features required for a space-flight-path sensor that is scalable directly to a sensor meeting the 3D wind mission requirements. We are awaiting delivery of the laser source (expected within the next few weeks). Once integrated the system is ready to commence ground validation testing against a well calibrated coherent detection DWL. Following ground testing the system will be installed in a WN-57 flight pallet and flown at high altitude in an autonomous operating mode. Flight validations will be accomplished by comparing OAWL wind profiles to multiple NOAA wind profiler network data for a variety of conditions along the flight path, and also against a ground-based DWL operated by NOAA near Boulder, CO. A successful test program will result in availability of an alternative "hybrid" architecture for the 3-D winds mission that promises to save significant cost, mass, and power, while offering the potential to combine 3-D winds and other important environmental missions [12].

References

[1] A Community Assessment and Strategy for the Future, NRC; Earth Science and Applications from Space: National Imperatives for the Next Decade and Beyond. The National Academies Press, 2007**.**

[2] Hardesty, et al, Providing global wind profiles – the missing link in today's observing system, 2005.

http://space.hsv.usra.edu/LWG/Splash%20Papers/Hardesty.pdf

[3] C. J. Grund, J. Howell, R. Pierce, and M. Stephens, "Optical Autocovariance Direct Detection Lidar for Simultaneous Wind, Aerosol, and Chemistry Profiling from Ground, Air, and Space Platforms", Paper 7312-37:SPIE Defense & Security Sensing Symposium; conference on Advanced Environmental, Chemical, and Biological Sensing Technologies VI, 2009

[4] M.J. Kavaya, G.J. Koch, J. Yu, B. Trieu, F. Amzajerdian, U.N. Singh, M. Petros, "IIP Update: A Packaged Coherent Doppler Wind Lidar Transceiver "Doppler Aerosol WiNd lidar (DAWN)" http://space.hsv.usra.edu/LWG/Jun06/Papers.jun06/Kavaya1.jun06.ppt

[5] Gentry, B.M., et al, Wind measurements with 355-nm molecular Doppler lidar, Opt. Let. , 25, 1231-1233, (2000).

[6] Grund, et al (2007): Optical Autocovariance Wind Lidar and Performance from LEO, 14th CLRC. Available from: http://space.hsv.usra.edu/CLRC/presentations.html.

[7] Schwiesow, and Mayor (1995): Coherent Optical Signal Processing for a Dop. Lidar using a Michelson Interferometer, OSA 1995 Tech. Dig. Series, 19, WA5-1 - WA5-4.

[8] Bruneau, D., (2001): Mach-Zehnder interferometer as a spectral analyzer for molec. DWL, Appl.Opt. 40, 391-399.

[9] Weimer, C., et al, (2007): Commissioning of the CALIPSO Payload, in publication, **SPIE 65550J-1**.

[10] Martin Endemann ADM-Aeolus: the first spaceborne wind lidar. SPIE Proceedings Vol. 6409, (2006).

[11] Courtesy of Bruce Gentry, NASA/GSFC.

[12] Grund, et al Supporting NOAA and NASA High-Performance space-based DWL objectives with a min. cost, mass, power, and risk approach employing OAWL. Feb 2008 Working group on Space-Based Lidar Winds, 2008: http://space.hsv.usra.edu/LWG/Index.html.

*